Springer

KSME

Journal of Mechanical Science and Technology 29 (3) (2015) 1085~1091
www.springerlink.com/content/1738-494x
DOI 10.1007/s12206-015-0220-0

# Long-term investigation of erosion behaviors on metal surfaces by impingement of liquid droplet with high-speed †

Duk Hyun Choi[1], Kyung Hoon Kim[1,*] and Hyung Joon Kim[2]

[1]*Kyunghee University, 1 Seocheon-dong, Gihung-gu, Yongin-Shi, Gyeonggi-do, 446-701, Korea*
[2]*Department of Mechanical and Aerospace Engineering, Seoul National University, 1 Gwanak-ro, Gwanak-gu, Seoul, 151-744, Korea*

(Manuscript Received April 10, 2014; Revised October 22, 2014; Accepted November 26, 2014)

**Abstract**

Understanding wall-thinning erosion of pipelines in nuclear or steam power plants is critically important for predicting and preventing human and material accidents. Wall thinning of pipelines in power plants occurs mainly by flow acceleration corrosion (FAC), cavitation erosion (C/E), and liquid droplet impingement erosion (LIE). Wall thinning by FAC and C/E has been well-investigated; however, LIE in plant industries has rarely been studied due to the experimental difficulty of setting up a long injection of highly pressurized air. We designed a long-term experimental system for LIE and investigated the behavior of LIE for three kinds of materials (A106B, SS400, A6061). The main control parameter was the air-water ratio (α), which was defined as the volumetric ratio of water to air (0.79, 1.00, 1.72). To clearly understand LIE, the spraying velocity ($v$) of liquid droplets was controlled larger than 160 m/s and the experiments were performed for 15 days. The surface morphology and hardness of the materials were examined every five days. Since the spraying velocity of liquid droplets and their contact area ($A_c$) on specimens were changed according to the air-water ratio, we analyzed the behavior of LIE for the materials using the impulse (I), which was defined as $I = (\alpha \times v) / A_c$. Finally, the prediction equations (the erosion rate) for the LIE of the materials were determined for the air-water ratios.

*Keywords*: Liquid droplet impingement erosion (LIE); Air-water ratio; Impulse; Erosion rate; Two phase nozzle

## 1. Introduction

The pipelines in nuclear and stream power plants suffer from time-dependent wall-thinning erosion [1-5] that leads to cracks and holes, ultimately causing the sudden fracture of pipelines. Based on the scale of plant systems, such accidents might result in tragic human injuries or huge economic loss. It is essential to predict and prevent the damage of pipelines in plant systems. Generally, wall thinning of pipelines in power plants occurs by flow acceleration corrosion (FAC) [6-8], cavitation erosion (C/E) [9-12], and liquid droplet impingement erosion (LIE) [13-17]. FAC occurs when the corrosion and dissolution of the surface oxide layer of carbon steels and low alloy steels are accelerated by fluidic flow in a pipeline. Wall thinning of pipelines by FAC usually happens along the whole surface of the pipe, causing large-sized fractures in large caliber pipelines. FAC has been studied extensively in the past, and many research centers are still actively investigating this type of corrosion. C/E is the damage of pipelines by the saturated pressure that is generated when cavitation bubbles pop at the neck of pipelines. C/E occurs locally and is currently suppressed by the designed shape of pipelines. LIE takes place when pipelines are damaged by the strong impulse induced when a droplet is mixed with a high-speed steam flow. LIE has been studied mainly in the aircraft industry to understand the damage of turbine blades from raindrops, but it has rarely been investigated in industrial plants. Some studies have been performed, but only under the constricted condition of short-time space (within 24 hours) and low impulses (less speed than 100 m/s) due to the difficult experimental setup for a long-term injection of highly-pressurized air [18-20]. These experiments limit the ability to predict fractures in pipelines by LIE since the detecting the cause and initiation of the erosion is critically important. An experimental investigation with a long-term scale and highly-pressurized air are therefore necessary, but it has not been accomplished yet.

We have developed an experimental system with a long injection of high-pressure air by using two compressors and a two-phase nozzle. Using this experimental system, we are able to investigate the behavior of LIE for several days and with high-speed spray of liquid droplet over 160 m/s. We use three kinds of materials (A106B, SS400, A6061) as a function of the air-water ratio (α), which is defined as the volumetric ratio of water to air. The air-water ratio is controlled from 0.79 to

*Corresponding author. Tel.: +82 1099849015, Fax.: +82 312028106
E-mail address: kimkh@khu.ac.kr
† Recommended by Associate Editor Simon Song

Table 1. Experimental condition.

| | |
|---|---|
| Air flux $Q_A$ [$m^3$/s] | $2.90 \times 10^{-5}$ |
| Water flux $Q_W$ [$m^3$/s] | $2.28 \times 10^{-5}$ |
| | $2.90 \times 10^{-5}$ |
| | $5.00 \times 10^{-5}$ |
| Air-water ratio $\alpha$ ($Q_W$ / $Q_A$) | 0.79 |
| | 1.00 |
| | 1.72 |
| Velocity $v$ [m/s] | 181 |
| | 175 |
| | 168 |
| Contact area $A_C$ [$mm^2$] | 452.16 |
| | 486.95 |
| | 538.31 |
| Impulse, $I$ $v \times \alpha / A_C$ [$10^5$/s·m] | $3.16 \times 10^5$ |
| | $3.60 \times 10^5$ |
| | $5.37 \times 10^5$ |

1.72. The results are analyzed by examining the impulse (I) at the surface of the materials. Finally, we determined the LIE erosion rate equations for the materials used in this study.

## 2. Experiments

### *2.1 Experimental system for a long-term continuous test with highly-pressurized air*

Based on the condition for the flux of water and air currently used in most plant systems, we designed and developed an experimental system that can be operated under long-time (several days) an extended time and high-speed spraying (over 160 m/s) condition. There are two kinds of erosion machines used worldwide: a whirl arm type (US, Bell Aerospace Company), and a disk rotary type (UK, Cambridge University). Those machines cannot provide a fluidic velocity larger than 100 m/s and only use water without air flow, so experimental investigations as a function of the air-water ratio are not impossible for these machines. However, the fluid in pipelines of nuclear or stream power plants usually includes air, so the air-water ratio is a critically important parameter to understand the erosion behavior of pipeline materials. For this reason, we used a two-phase nozzle to perform our experiments as a function of the air-water ratio. To be more specific, we designed our experimental set-up to be able to simultaneously control the flux and the pressure of water and air, as well as the distance between the specimen and the nozzle. As shown in Fig. 1(a), the experimental system consists of (i) two air compressors, (ii) a compressed air reservoir tank, and (iii) a test stage. The detailed design of the experimental setup is illustrated in Fig. 1(b). The air compressors (1,2) are connected together in parallel, and operated in the range of 6.5 - 8.5 bar, which is the condition that the pressured air and liquid form two-phase

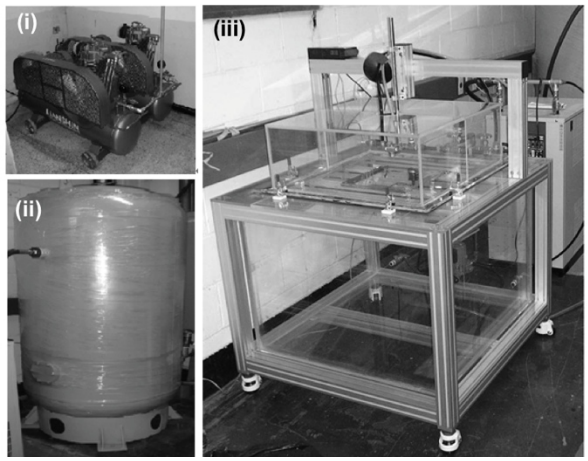


(a)

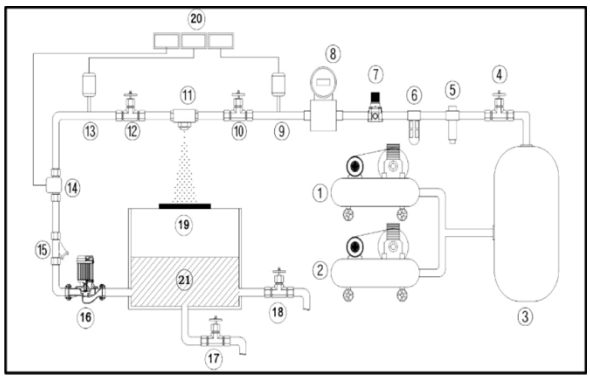


(b)

Fig. 1. Experimental set-up: (a) photograph for the core instruments of (i) two air compressors, (ii) a compressed air reservoir tank, and (iii) a test stage; (b) schematic diagram of experimental apparatus: (1) No.1 air compressor, (2) No.2 air compressor, (3) compressed air reservoir tank, (4) main air control valve, (5) refrigerated air dryer, (6) air filter, (7) regulator, (8) air flowmeter, (9) air pressure gauge, (10) air flow control valve, (11) air atomizing nozzle, (12) water flow control valve, (13) water pressure gauge, (14) water flow meter, (15) water strainer, (16) pump, (17) drain valve, (18) feed valve, (19) specimen, (20) display set box, (21) water tank.

fluid. Air produced from the air compressors was first saved in the compressed air reservoir tank (3), and then passed through the dryer (5) to cool to 15°C and to dry, leading to the removal of foreign matters. Finally, the air was supplied to the test stage with a gauge pressure of 5.5 bar.

The test stage was designed to simulate real field condition for LIE by using a two-phase nozzle (11), which is an internal mixing type. Air was provided into the middle of the nozzle, and water was supplied to the other sides of the nozzle. The regulator (7) at the end of the air flow control valve (10) was used to maintain the air flux that was provided by the air compressors. The water flux supplied by the pump (16) was controlled by the water flow control valve (12). To monitor the flux of air and water, flow meters (8, 14) and a display set (20) were installed. The feed and drain valves (17, 18) were used to control the amount of water in the water tank (21) so that the

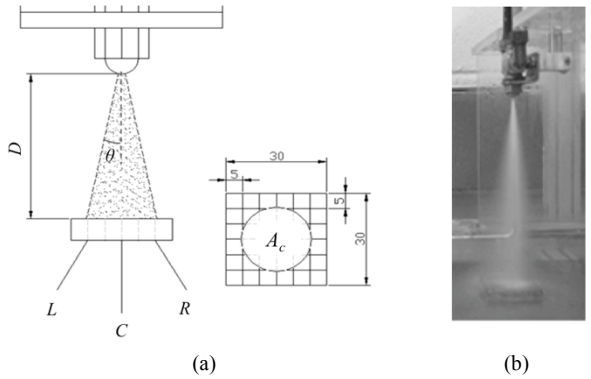


(a) (b)

Fig. 2. (a) Schematic arrangement for the two-phase nozzle and a specimen. The contact area ($A_c$) of liquid droplets on the specimen was determined by measuring the spraying angle (θ) of the injecting droplets. The distance (D) of the specimen from the nozzle was fixed to 45 mm; (b) Photographic image for spraying liquid droplet during the experiments.

water lost during the experiment was able to be refilled.

### *2.2 Experimental conditions*

Fig. 2(a) shows the schematic arrangement for the two-phase nozzle and a specimen. The distance of the specimen from the nozzle was fixed at 45 mm, which is the optimized distance for the rebounded droplets not to have an effect on the specimen [21]. The specimen size was 30 × 30 $mm^2$. We prepared the specimens by cutting pipelines that are actually used in the industry, which include two kinds of carbon steel (A106B and SS400) and aluminum (A6061). A106B contains a high level of carbon steel which is also widely used and is the material used most often in industrial plants; SS440 is a reference material for a low carbon steel. A6061 was selected as a representative material for non-ferrous metals. The contact area ($A_c$) of liquid droplets on the specimen was determined by measuring the spraying angle (θ) of the injected droplets from photographic images during the experiments, as shown in Fig. 2(b). The contact area of liquid droplets on the specimen is an important parameter to quantitatively analyze the LIE behavior since this contact area can alter the impulse (I).

The main parameter for our long-term LIE experiments is the volume ratio of water and air per time, referred to the air-water ratio (α) in this study. As shown in Table 1, the maximum air flux $Q_A$ ($m^3/s$) was determined to be 2.90 × 10-5 $m^3/s$ based on the performance of the air compressors, and the water flux $Q_W$ ($m^3/s$) was determined by considering different air-water ratios. To analyze the behavior of the LIE in terms of impulse, we needed to measure the velocity ($v$) of the liquid droplets according to the air-water ratio, since the velocity was significantly affected by the air-water ratio. The velocity was measured in the range of the air-water ratio from 0 to 2 by both a pitot-tube and bi-directional flow tube, as shown in Figs. 3(a)-(d). Since the bi-directional flow tube was designed by McCarrey to measure the local velocity of a flame with complex fluidic directions, it was adequate to monitor the

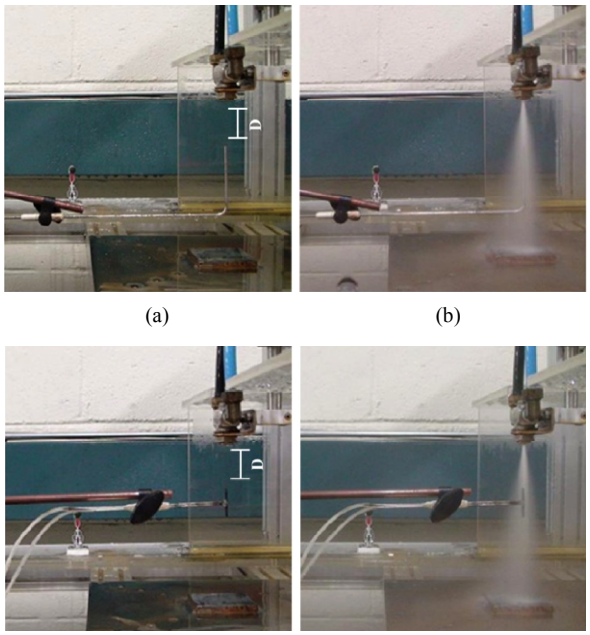

(a) (b)

(c) (d)

Fig. 3. (a)-(b) Photographic images for velocity measurement by a pitot-tube; (c)-(d) Photographic images for velocity measurement by a bi-directional flow tube. The distance (D) between the measuring position of the tubes and the two-phase nozzle was the same.

velocity of the liquid droplets. The measurement positions were the left (L), right (R), and center (C) positions at the same distance (D) from the nozzle, as shown in Fig. 2(a). To determine the velocity, we used the following equation:

$$V = k\sqrt{\frac{2\Delta P}{\rho}}\,. \tag{1}$$

In the LIE test, we applied the air-water ratios of 0.79, 1, and 1.72 to the three kinds of specimens, and measured the weight difference and the hardness every five days, and continued the test for 15 days. The surface was investigated by photographs and scanning electron microscopy (SEM) images. Because the LIE might be similar according to the radial positions from the center of a specimen, the SEM images were taken from the highly damaged regions, which were the solid circles on the photographic images, as shown in Fig. 5(a). The weight change was obtained by using a digital scale with a resolution on the order of $10^{-4}$ g. The hardness was determined with a Vickers hardness tester and measured at the 16 different positions.

## 3. Results and discussion

### *3.1 Impulse in the experiment*

Fig. 4(a) presents the velocity of liquid droplets according to the air-water ratio. The results measured from the two tubes similarly showed that the velocity decreased as the air-water ratio increased. The velocity was in the range of 165 m/s to 231 m/s, which is suitable for investigating the behavior of

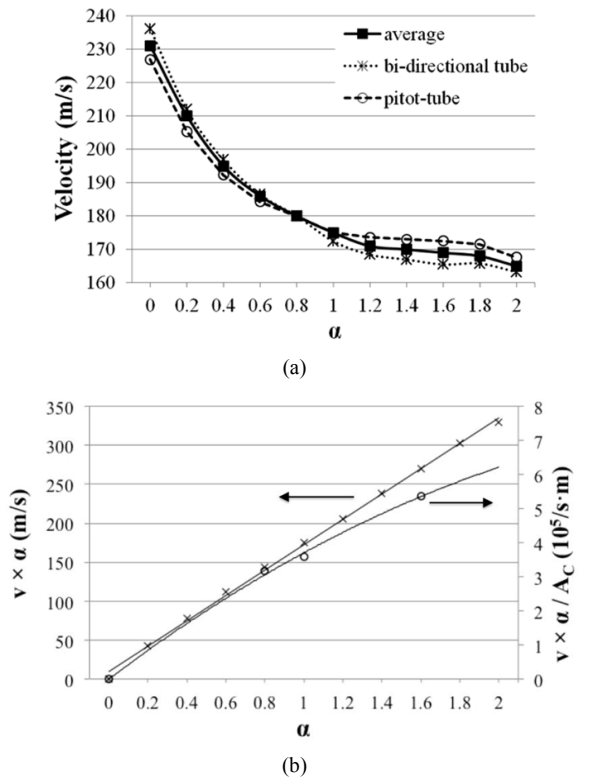


Fig. 4. (a) Velocity of liquid droplets according to the air-water ratio; (b) proposed impulse of the liquid droplets according to the air-water ratio.

long-term LIE since the LIE of a two-phase fluid main-ly occurs when the liquid droplet velocity is larger than the critical velocity (90 m/s for a carbon steel and 30 m/s for a general steel) [23]. Consequently, these results suggest that the long-term LIE behavior of plant materials can be understood by using our experimental system.

In this study, the main parameter was the air-water ratio, but the actual factor for the LIE might have been the impulse of the liquid droplets on the specimens. Impulse is defined by the momentum change of an object, and the momentum is the product of the mass and the velocity of the object. In our experiments, the total mass of liquid droplets increased as the air-water ratio increased. However, the mass of the liquid droplets before and after the impingement test did not change; velocity was the only factor that changed. The initial velocity of the liquid droplets before impingement was much higher after the impingement, so we could assume that the impulse of the liquid droplets was mainly affected by the product of the air-water ratio and the initial velocity of the liquid droplets ($\alpha \times v$). Furthermore, the impulse on specimens decreases when the contact area ($A_c$) of the liquid droplets on the specimen increases. Finally, we assume that the impulse from the liquid droplets in this experiment is $\alpha \times v / A_c$ (i.e., $I \propto \alpha \times v / A_c$). Fig. 4(b) shows the impulse behavior of the liquid droplets according to the air-water ratio. When the contact area was not considered, $\alpha \times v$ increased linearly with $\alpha$.

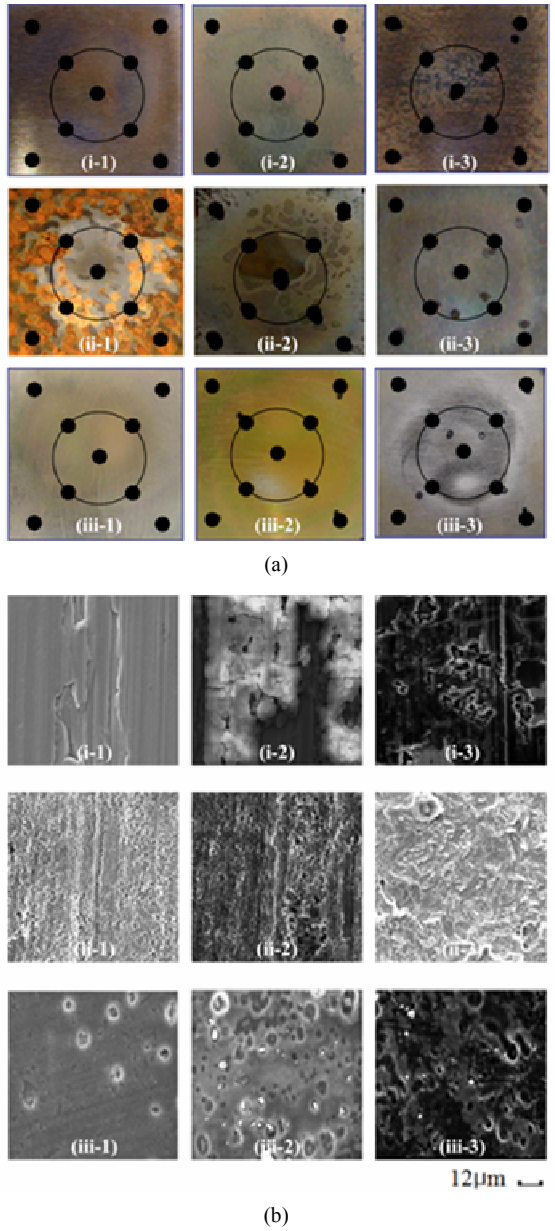


Fig. 5. Surface characterizations: (a) Photographs for the specimens ((i) A106B, (ii) SS400, (iii) A6061) for every 5 day; (b) SEM images for the specimens after LIE tests for 15 days at the position of the solid circle in the photographic images.

However, we measured the contact area of liquid droplets for three air-water ratios, which are shown in Table 1. Based on these contact areas, we again investigated the impulse as a function of $\alpha \times v / A_c$, as shown in Fig. 4(b). Consequently, the impulse of liquid droplets increased non-linearly with the air-water ratio. We subsequently applied this result to analyze the LIE behavior on the specimens.

### *3.2 Surface characterizations*

After the LIE was tested for 15 days, discoloration of the

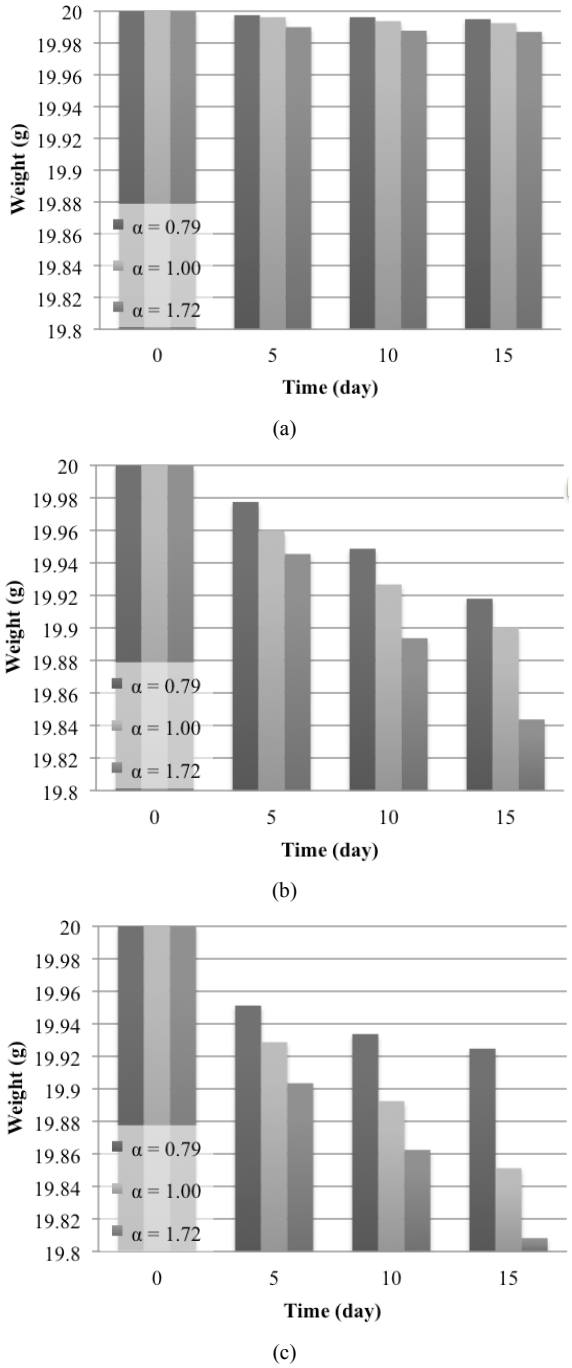


Fig. 6. Weight change according to the air-water ratio and test time for (a) A106B; (b) SS400; (c) A6061.

specimens by corrosion was clearly observed for all the specimens, as shown in Fig. 5(a). Furthermore, the impulse by the liquid droplets was radially symmetric, so the erosion appeared differently in the radial directions (see the circles in the photographs). In particular, the median position of the specimens showed less erosion than the other positions due to the flow patterns from our two-phase nozzle. Fig. 5(b) presents the SEM images at the solid circle in Fig. 5(a), at which the highest erosion occurred. As these figures indicate, the surface

Table 2. Hardness results according to the air-water ratio and experimental time.

| Material | Air-water ratio, $\alpha$ | HV changes | | | |
|---|---|---|---|---|---|
| | | Initial | 5 days | 10 days | 15 days |
| A106B | 0.79 | 198 | 172 | 151 | 142 |
| | 1 | | 168 | 150 | 140 |
| | 1.72 | | 170 | 152 | 143 |
| SS400 | 0.79 | 204 | 168 | 121 | 108 |
| | 1 | | 170 | 118 | 99 |
| | 1.72 | | 164 | 119 | 100 |
| A6061 | 0.79 | 107 | 104 | 100 | 98 |
| | 1 | | 105 | 103 | 100 |
| | 1.72 | | 105 | 104 | 103 |

erosion by the liquid droplet impingement progressed for all the specimens as the air-water ratio increased. Furthermore, the erosion behaviors were clearly different among the materials. In case of the carbon steels A106B and SS440, the erosion process could be divided into two steps: first, the formation of line cracks in one direction, and then main erosion by the delamination of layers, as shown in Figs. 5(b-i) and 5(b-ii). For aluminum A6061, the initial erosion formed pores, which was followed by the growth of the pores and then the delamination of the material.

### *3.3 Weight change analysis*

To directly evaluate the LIE, we measured the reduction of the weight for the specimens, as shown in Fig. 6. For the specimen of A106B, the erosion by liquid droplet impingement was minimal due to the high erosion resistance of the high carbon steel, even though the experimental erosion condition was much more severe than real field conditions (Fig. 6(a)). As shown in Fig. 5(a-ii), high carbon containing SS440 eroded much more due to the liquid droplet impingement (Fig. 6(b)). Over time, high carbon steels showed less reduction of weight (Fig. 6(a)) than low carbon steel and aluminum cases (Figs. 6(b) and (c)). In all cases as the air-water ratio increased, the reduction rate of weight increased. This process might be attributed to the fact that the erosion of carbon steels is accelerated by high air-water ratios due to a number of line cracks. Once cracks form, high-pressure air and water can quickly and easily infiltrate the inside of the material. As a result, the erosion of the surface and the inside occurs simultaneously, and thus accelerates erosion. In case of aluminum A6061, the reduction rate of the weight due to LIE was initially high, but it gradually decreased over time. The reduction rate of weight also decreased with the air-water ratio (Fig. 6(c)). This result might stem from the localized formation of pores and the instant formation of an oxide layer on the surface of the aluminum. Even though, the total reduction of weight was the largest for the A6061 due to its low mechanical property; however, the LIE behavior was clearly different for aluminum and the

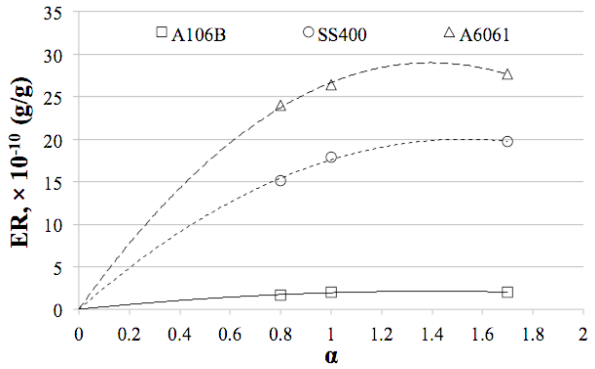


Fig. 7. Erosion rate as a function of the air-water ratio for the specimens.

carbon steels (Fig. 6(c)).

### *3.4 Hardness analysis*

Table 2 shows the average values of the hardness of the specimens under different air-water ratios during the test period of 15 days. Interestingly, the hardness rarely changed by the different air-water ratio during the same test. This phenomenon can be understood by the fact that the hardness is a bulk property in the depth direction. Although the surface erosion was quicker with higher air-water ratios, the mechanical property in the depth direction did not change because the deterioration of material in the depth direction is significantly dependent on time by infiltrating the air and water. During the test, the carbon steels A106B and SS400 exhibited large changes in hardness, but the aluminum A6061 showed only a minute change. Similar to the reduction rates of the specimen weight, these changes in hardness might stem from the different behaviors of surface erosion by LIE. Since the carbon steels showed many line cracks, the inside of the materials was easily deteriorated by LIE, thus leading to significant decreases in the hardness. On the other hand, A6061 made localized pores and instantly oxidized the surface, thereby preventing the fast corrosion of the inside causing only a small change in the hardness.

### *3.5 Erosion rate for LIE*

Based on the weight reduction of the specimens according to the erosion time, we estimated the erosion rate (*ER*) using Eq. (2), in which the *ER* can be determined by the ratio of the weight reduction of the specimen ($W_{\text{specimen}}$) to the weight of the injected liquid droplet ($W_{\text{erodent}}$).

$$ER = \frac{W_{specimen}}{W_{erodent}}. \tag{2}$$

The results are shown in Fig. 7. As the air-water ratio increased, the *ER*s for the specimens were saturated for α from 0 to 1.72. The *ER* was the largest for A6061 and the smallest for the A106B. By using the *ER* as a function of α in Fig. 7, the relationship between the air-water ratio and *ER* was determined. Eqs. (3)-(5) give these relationships for A106B, SS400, and A6062, respectively. Note that these equations are only valid for air-water ratios from 0 to 1.72.

$$ER = -1.0868 \cdot \alpha^2 + 3.0395 \cdot \alpha \tag{3}$$

$$ER = -8.5003 \cdot \alpha^2 + 26.074 \cdot \alpha \tag{4}$$

$$ER = -14.898 \cdot \alpha^2 + 41.561 \cdot \alpha\,. \tag{5}$$

## 4. Conclusions

We have designed and developed an experimental system to investigate the behavior of long-term LIE of pipelines used in plant industries with high-speed liquid droplets. In previous reports, the behavior of LIE was only studied for a short time span and under a mild condition compared to the real field condition. In our experimental system, we were able to investigate the behavior of pipeline LIE for long time span and under a relatively severe condition. The results of our experiment showed that the erosion rates of carbon steels increased linearly with the erosion time, but the erosion rate of aluminum was saturated over time. These different behaviors can be understood by the different crack initiation for the specimens. In the carbon steels, many line cracks were initially formed, but in aluminum, localized pores were formed. Furthermore, the mechanical hardness changed significantly in the carbon steels, but it changed marginally in the aluminum. These differences were also attributed to the initial crack formation and the different corrosion properties in the inside of the specimens. Finally, we determined the erosion rate (*ER*) according to the air-water ratio for each specimen, which may provide valuable data to predict and prevent damage to the pipelines by LIE in plant industries.

## Acknowledgment

This work was supported by National Research Foundation of Korea (NRF) grant funded by the Korea government (MEST) (N0. 20111793).

## Nomenclature

| | |
|---|---|
| $\alpha$ | : Air-water ratio |
| $I$ | : Impulse |
| $A_c$ | : Contact area |
| $\theta$ | : Spraying angle |
| $Q_A$ | : Air flux |
| $Q_W$ | : Water flux |
| $v$ | : Velocity of liquid droplets |
| $\Delta P$ | : Pressure difference |
| $\rho$ | : Density of air |
| $k$ | : Calibration factor |
| $ER$ | : Erosion rate |

## References


[1] NRC, *Thinning of pipe walls in nuclear power plant*, Bulletin 87-01 (1987).

[2] D. H. Lister and L. C. Lang, A mechanistic model for predicting flow-assisted and general corrosion of carbon steel in reactor primary coolants, *International Conference on Water Chemistry in Nuclear Reactor Systems*, Avignon (2002).

[3] P. Alto, Recommendations for controlling cavitation, flashing, liquid droplet impingement and solid particle erosion in nuclear power plant piping systems, *EPRI*, 1011231 (2005).

[4] KEPCO, Monitoring corrosion in nuclear piping system, *Topical Report TR.96NW01.J1999.346* (1998).

[5] Y. Kim, J. Yoo and M. Lee, Optimal design of spaced plates under hypervelocity impact, *JMST*, 26 (5) (2012) 1567-1575.

[6] V. K. Chexal and J. S. Horowitz, Flow-assisted corrosion in carbon steel piping parameters and influences, *EPR*, 1 (1989).

[7] NRC, *Rupture in extraction steam piping as a result of flow-accelerated corrosion* (1997) Notice 97-84.

[8] S. Chun and H.-S. Kwon, Use of Wigner-Ville transformations for fluid particles in laser Doppler flow accelerometry, *JMST*, 26 (3) (2012) 857-867.

[9] J. Ducreaux, Corrosion-erosion of steels in high temperature water and wet steam, Paper No. 14, *Electricite de France*, Les Renardieres France (1982).

[10] P. Berge et al., *Water chemistry of nuclear reactor systems 2*, London, British Nuclear Energy Society (1981) 124.

[11] J. Ducreaux, *Water chemistry of nuclear reactor system 3*, Vol. 1, London, British Nuclear Energy Society (1983) 227.

[12] H. Sun, Numerical study of hydrofoil geometry effect on cavitating flow, *JMST*, 26 (8) (2012) 2535-2545.

[13] W. Kastner, K. Riedle and H. Trats, Experimental inspections on material loss due to Erosion-Corrosion, *VGB Kraftweeks Technik*, 64 (5) (1984) 411-243.

[14] Y. Y. Liu and Natesan, Oxidation-erosion of metals and alloys: Models, verification and prediction, *Surface and Coatings Technology*, 36 (1988) 407-417.

[15] L. Pawlowsk, *The science and engineering of thermal spray coatings*, Wiley, New York (1995).

[16] M. C. Rochester and J. H. Brunton, Influence of physical properties of the liquid on the erosion of solids, *ASTM STP*, 567 (1974) 128-151.

[17] S. Park and G. Jeun, Calculation of water droplet impingement using the coupled method of rigid body dynamics and the moving particle semi-implicit method, *JMST*, 25 (11) (2011) 2787-2794.

[18] H. Keller, Corrosion and erosion problems in saturated-steam turbines, *AIM Conf*., Liege, Belgium (1978) 22-28.

[19] P. Berge, J. Ducreux and P. Saint, Effects of chemistry on corrosion-erosion of steels in water and wet steam, *Water Chemistry 2*, BNES, 2 (1980) 19-23.

[20] S. M. Wiederhorn and B. R. Lawn, Strength degradation of glass impacted with shape particles, *J. Am. Ceram. Soc*., 62 (1-2) (1979) 66-70.

[21] D. Choudhury, *Introduction to the renormalization group method and turbulence modeling*, Fluent Inc., Technical Memorandum TM-107 (1993).

[22] B. J. Yun, Development of an average bi-directional flow tube for the measurement of single and two phase flow rate, *KFMA* (2004) 172-179.

[23] M. G. Fontana, *Corrosion engineering*, 3rd ed., McGraw Hill (2008) 25, 70-71, 95-97, 485-487.


**Kyung Hoon Kim** serves as a professor in Kyung Hee University. Professor Kim's research interests include turbulence, pipe flow & flow visualization.